

Inositol Hexaphosphate Suppresses Growth and Induces Apoptosis in Prostate Carcinoma Cells in Culture and Nude Mouse Xenograft: PI3K-Akt Pathway as Potential Target

Mallikarjuna Gu,¹ Srirupa Roy,¹ Komal Raina,¹ Chapla Agarwal,^{1,2} and Rajesh Agarwal^{1,2}

¹Department of Pharmaceutical Sciences, School of Pharmacy, and ²University of Colorado Cancer Center, University of Colorado-Denver, Aurora, Colorado

Abstract

Constitutive activation of phosphoinositide 3-kinase (PI3K)-Akt pathway transmits growth-regulatory signals that play a central role in promoting survival, proliferation, and angiogenesis in human prostate cancer cells. Here, we assessed the efficacy of inositol hexaphosphate (IP6) against invasive human prostate cancer PC-3 and C4-2B cells and regulation of PI3K-Akt pathway. IP6 treatment of cells suppressed proliferation, induced apoptosis along with caspase-3 and poly(ADP-ribose) polymerase (PARP) cleavage, and inhibited constitutive activation of Akt and its upstream regulators PI3K, phosphoinositide-dependent kinase-1 and integrin-linked kinase-1 (ILK1). Downstream of Akt, IP6 inhibited the phosphorylation of glycogen synthase kinase-3 α/β at Ser^{21/9} and consequently reduced cyclin D1 expression. Efficacy studies employing PC-3 tumor xenograft growth in nude mice showed that 2% (w/v) IP6 feeding in drinking water inhibits tumor growth and weight by 52% to 59% ($P < 0.001$). Immunohistochemical analysis of xenografts showed that IP6 significantly reduces the expression of molecules associated with cell survival/proliferation (ILK1, phosphorylated Akt, cyclin D1, and proliferating cell nuclear antigen) and angiogenesis (platelet endothelial cell adhesion molecule-1 or CD31, vascular endothelial growth factor, endothelial nitric oxide synthase, and hypoxia-inducible factor-1 α) together with an increase in apoptotic markers (cleaved caspase-3 and PARP). These findings suggest that, by targeting the PI3K-ILK1-Akt pathway, IP6 suppresses cell survival, proliferation, and angiogenesis but induces death in prostate cancer cells, which might have translational potential in preventing and controlling the growth of advanced and aggressive prostate cancer for which conventional chemotherapy is not effective. [Cancer Res 2009;69(24):9465-72]

Introduction

In the United States, prostate cancer is the most common malignancy and the second leading cause of cancer-related deaths in men (1). Despite decades of research and treatment advances, androgen withdrawal is the only effective therapy for advanced prostate cancer patients (1). However, prolonged androgen deprivation results in relapse and ultimately leads to more aggressive androgen-independent prostate cancer stage in almost all patients (1). Several nonhormonal agents have been evaluated in patients with hormone-refractory

prostate cancer; however, they have limited antitumor activity with an objective response rate of <20% and no demonstrated survival benefit (2, 3). These caveats highlight the urgent need for additional strategies and the agents to effectively manage and control clinical prostate cancer.

Phosphoinositide 3-kinase (PI3K) is activated in response to diverse mitogenic signals and catalyzes the formation of second messenger lipid phosphatidylinositol-3,4,5-triphosphate. Binding of phosphatidylinositol-3,4,5-triphosphate to pleckstrin homology domain of Akt results in its recruitment to plasma membrane, where it is activated by phosphorylation at Thr³⁰⁸ by phosphoinositide-dependent kinase-1 (PDK1; ref. 4). However, full activation of Akt also requires phosphorylation at Ser⁴⁷³, which is regulated by various kinases. Integrin-linked kinase-1 (ILK1) is a PI3K-dependent effector of integrin-mediated cell adhesion and has been shown to phosphorylate Akt at Ser⁴⁷³ both *in vitro* (5, 6) and *in vivo* (7). On activation, Akt regulates the function of various molecules involved in diverse cellular events including proliferation and survival (8). Glycogen synthase kinase-3 (GSK3) α/β is an important target of Akt and is regulated by inactivating phosphorylation at Ser²¹ of GSK3 α and Ser⁹ of GSK3 β (9, 10). Accumulation of GSK3 β in the nucleus mediates phosphorylation, nuclear export, and subsequent ubiquitin-dependent degradation of cyclin D1, thereby linking the PI3K-Akt pathway with cell proliferation (11). During prostatic tumorigenesis, phosphatase and tensin homologue (PTEN) is most commonly mutated, which causes constitutive activation of the PI3K-Akt pathway and thereby renders uncontrolled proliferative potential and apoptosis resistance to prostate cancer cells (12). About 50% of all human cancers exhibit PDK1 overactivation leading to increased Akt phosphorylation; inhibition of this protein kinase by small molecules results in effective inhibition of cancer cell proliferation (13). Overexpression of ILK1 in epithelial cells induces anchorage-independent cell growth, suppresses anoikis, and promotes tumor formation *in vivo*; its expression in human prostate tissues increases with disease progression and is inversely correlated with patient survival (14, 15). Moreover, in prostate cancer cells, ILK1 regulates hypoxia-inducible factor-1 α (HIF-1 α) expression and thereby stimulates vascular endothelial growth factor (VEGF) production resulting in endothelial cell migration and tumor angiogenesis (16). The integrative signaling of PI3K-Akt pathway underlines its importance in tumor progression and it is thus logical that the agents, which target the members and/or regulators of this pathway, hold significant promise in controlling the advancement of prostate cancer to more aggressive phenotypes.

Inositol hexaphosphate (IP6) is a naturally occurring polyphosphorylated carbohydrate mostly present in high-fiber diets (cereals, legumes, nuts, and soybean) and also in almost all plant and mammalian cells (17). IP6 has been consumed as an oral nutrient supplement for over a decade and is recognized for various

Requests for reprints: Rajesh Agarwal, University of Colorado-Denver, C238-P15, Research 2, 12700 East 19th Avenue, Room 3121, Aurora, CO 80045. Phone: 303-724-4055; Fax: 303-724-7266; E-mail: Rajesh.Agarwal@UCDenver.edu.

©2009 American Association for Cancer Research.
doi:10.1158/0008-5472.CAN-09-2805

health benefits without any toxicity in humans (17, 18). IP6 is rapidly absorbed by cells and metabolized into its lower phosphate forms, which regulate various cellular events (17, 18). Several studies by us and others have shown that IP6 plays an important role in cell proliferation, differentiation, and apoptosis in *in vitro* studies and inhibits tumor growth and progression *in vivo* without any toxic effects in various animal tumor models including prostate cancer (17–24). These promising reports prompted us to investigate whether antitumor efficacy of IP6 is mediated via inhibition of PI3K-Akt pathway, the most commonly deregulated cellular signaling cascade in prostate cancer. Our results show for the first time that signaling molecules in PI3K-Akt pathway are the primary molecular targets of IP6 for mediating its anticancer efficacy against PC-3 cells in terms of proliferation, survival, and angiogenesis under both *in vitro* and *in vivo* conditions.

Materials and Methods

Cell culture and reagents. PC-3 cells were from the American Type Culture Collection and C4-2B cells from ViroMed Laboratories. Cells were maintained under standard cell culture conditions. RPMI 1640, heat-inactivated fetal bovine serum, and penicillin-streptomycin were from Invitrogen. IP6 (sodium salt hydrate from rice) and antibody for β -actin were from Sigma. Antibodies for ILK1, cleaved poly(ADP-ribose) polymerase (PARP), cleaved caspase-3, total and phosphorylated forms of PI3K (p85 subunit), PDK1, Akt, and GSK3 α/β were from Cell Signaling Technology. CD31, VEGF, and endothelial nitric oxide synthase (eNOS) antibodies were from Abcam. Anti-cyclin D1 was from Neomarker. Anti-proliferating cell nuclear antigen, streptavidin-conjugated horseradish peroxidase, and N-universal negative control mouse or rabbit antibody were from Dako. Blocking buffer and anti-mouse and anti-rabbit secondary antibodies for Western immunoblotting were from LI-COR Biosciences. CoCl₂-stimulated COS7 nuclear extract was from Active Motif.

Cell growth and death and apoptosis assays. Cells were plated at 5,000/cm² in 60 mm plates overnight and then treated with 2 mmol/L IP6. At desired times, cells were harvested by brief trypsinization and

counted using a hemocytometer. Trypan blue dye exclusion was used to differentiate between live and dead cells. For apoptosis, internucleosomal DNA fragmentation was quantitatively assayed in IP6-treated PC-3 cells by antibody-mediated capture and detection of cytoplasmic mononucleosome and oligonucleosome associated histone-DNA complexes (Cell Death Detection ELISA Plus kit; Roche Diagnostics) following vendor' protocol.

Western immunoblotting. PC-3 and C4-2B cells at 50% to 60% confluency under standard culture conditions were treated with 2 mmol/L IP6 in fresh medium for 6, 12, and 24 h. Whole-cell or tumor tissue lysates were prepared as described earlier (19, 22) and 40 to 60 μ g protein per sample were denatured with 2 \times sample buffer and resolved on 8%, 12%, or 16% Tris-glycine gels. Separated proteins were transferred onto nitrocellulose membrane by Western blotting, and membrane was blocked for 1 h in Odyssey blocking buffer and then incubated with specific antibodies and with anti- β -actin for loading control followed by either goat anti-rabbit 800 or goat anti-mouse 680 secondary antibodies or both (both at 1:5,000) for 45 min. After the final wash, membranes were scanned using the Odyssey Infrared Imager (84 μ m resolution, 0 mm offset with medium or high quality; LI-COR Biosciences).

Animals and tumor xenograft study. Athymic (*nu/nu*) male nude mice (5–6 weeks old) were obtained from the National Cancer Institute and fed with sterilized AIN-76A rodent purified diet (Dyets) and water *ad libitum*. All procedures involving animals and their care were approved by the Institutional Animal Care and Use Committee of the University of Colorado-Denver. The mice were s.c. injected with \sim 2 million PC-3 cells mixed with equal volume of Matrigel (BD Biosciences) on the flank region of each mouse. After 1 week, only healthy animals having approximately equal tumor burden were selected carefully and distributed into three groups of 10 animals each. The first group served as control and fed with autoclaved drinking water, whereas the second and third groups were fed with 1% and 2% (w/v) IP6 in drinking water for 7 weeks. Animals were monitored for their water and diet consumption, weight gain, and tumor growth profiles twice a week for 7 weeks. Tumor volume was calculated by the formula: $0.5236 L_1 (L_2)^2$, where L_1 is the long axis and L_2 is the short axis of the tumor (23). At the end of the seventh week, animals were euthanized, the tumors were excised and weighed, and a small part of the tissue was fixed in buffered formalin and the remainder was snap-frozen in liquid nitrogen.

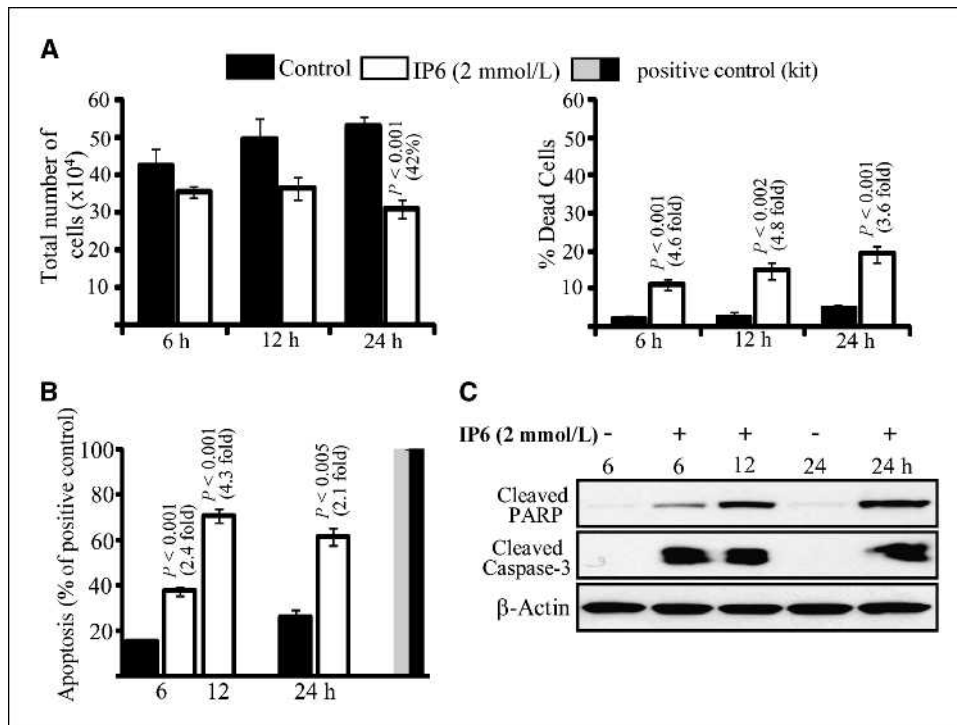


Figure 1. IP6 inhibits growth and induces apoptosis in PC-3 cells. PC-3 cells were treated with 2 mmol/L IP6 in complete medium for 6, 12, and 24 h and thereafter processed and analyzed as described in Materials and Methods. A, total cell number and percentage of cell death was determined by trypan blue dye exclusion assay. B, percentage of apoptotic cell population was detected by ELISA cell death assay. C, effect of IP6 on apoptotic markers cleaved PARP and cleaved caspase-3, as determined by Western blot analysis. In each case, membranes were simultaneously incubated with β -actin (loading control) and scanned with Odyssey Infrared Imager (84 μ m resolution, 0 mm offset with medium or high quality).

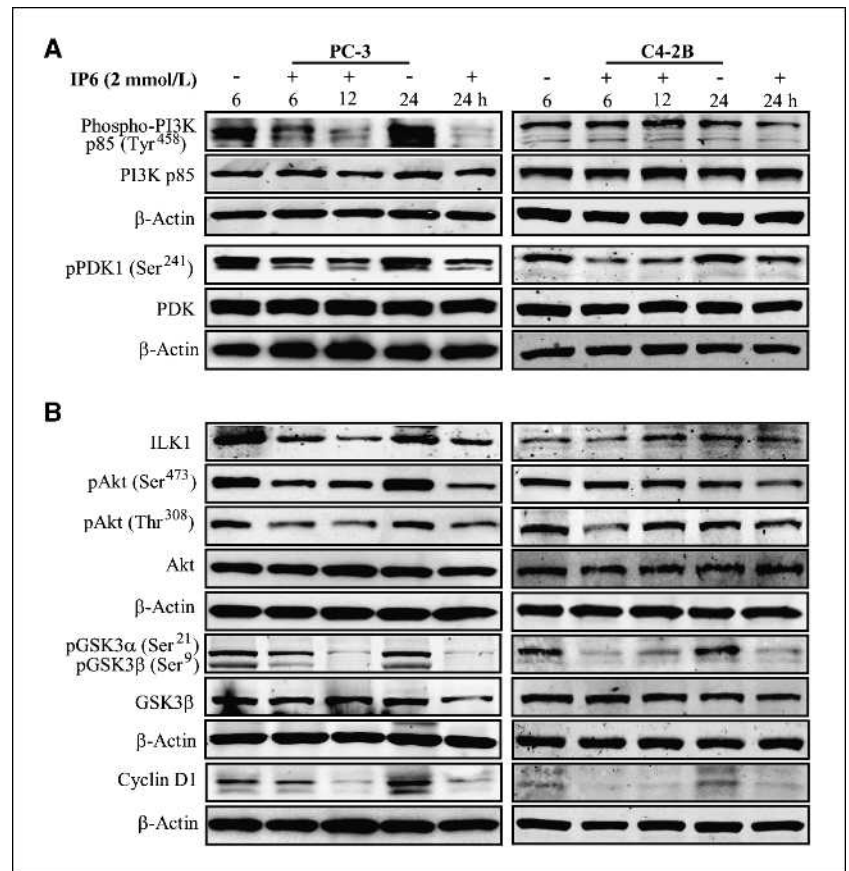


Figure 2. IP6 decreases phosphorylation or expression of signaling molecules in PI3K-PDK1-Akt axis in PC-3 and C4-2B cells. After specific treatments, cells were collected at 6, 12, and 24 h, cell lysates were prepared, and Western blotting was done to analyze the effect of IP6 on the expression of (A) phosphorylated and total PI3K and PDK1 and (B) ILK1, phosphorylated and total Akt at Ser⁴⁷³ and Thr³⁰⁸, GSK3 α / β (Ser^{9/21}), and cyclin D1 as detailed in Materials and Methods.

Immunohistochemical analysis and quantification. Tumor samples were processed for immunohistochemical analysis as described earlier (22–25), and sections were incubated overnight with specific antibodies for ILK1 (1:100), pAkt (Ser⁴⁷³; 1:50), cyclin D1 (1:250), CD31 (1:500), VEGF (1:500), or eNOS (1:250) and then with corresponding biotinylated secondary antibody, streptavidin, and 3,3'-diaminobenzidine. Negative controls were incubated only with universal negative control antibodies under identical conditions, processed, and mounted (25). Microscopic immunohistochemical analyses were done with a Zeiss AxioScop 2 microscope (Carl Zeiss). Quantification for nuclear pAkt (Ser⁴⁷³) and cyclin D1-positive cells was done in five arbitrarily selected fields/tumor samples at $\times 400$ magnification and data are represented as the number of positive (brown) cells $\times 100$ / total number of cells. Positive tumor microvessels were counted at $\times 400$ in five arbitrarily selected fields/tumor and the data are presented as number of CD31⁺ microvessels / $\times 400$ microscopic field for each group. Expression of pAkt (Ser⁴⁷³), ILK1, VEGF, and eNOS within the cytoplasm was subjectively graded and quantified as 0, 1, 2, 3, 4, and 5 representing not detectable, weak, moderate, strong, and very strong staining, respectively, and the average of five arbitrary fields/tumor at $\times 400$ magnification was quantified. Microscopic images were taken by AxioCam Mrc5 camera at $\times 400$ magnification and processed by AxioVision 4.6 (Carl Zeiss Microimaging; ref. 25).

Electrophoretic mobility shift assay. Nuclear extracts from PC-3 xenograft tumor tissues from all three groups were prepared as described earlier (25). The electrophoretic mobility shift assay was conducted as per vendor's protocol (LI-COR Biosciences) by adding 8 μ g nuclear protein extract to the reaction mixture containing 10 \times DNA-binding buffer, 2.5 mmol/L DTT/2.5% Tween 20, 1 μ g/ μ L poly(deoxyinosinic-deoxycytidylic acid), 1% NP-40, 50% glycerol, 0.5 μ g/ μ L sheared salmon sperm DNA, and 50 nmol/L HIF-1 IRDye end-labeled consensus oligo 5'-AGCTTGCCCTACGTGCTGTCTCAGA-3' and 3'-TCGAACGGGATGCACGACAGAGTCT-5' (nucleotides in boldface indicate HIF-1 binding motif). CoCl₂-treated COS7 nuclear extract served as positive control. Mutant HIF-1 IRDye

end-labeled oligos 5'-TCTGTAAAAAGACCACACTCACCTC-3' and 3'-AGACATTTCTGGTGTGAGTGGAG-5' were used to compete with the wild-type HIF-1 binding sequence to establish the specificity of DNA-protein complex. Following incubations, the resulting complexes were resolved on 4% to 16% native bis-Tris gel at 100 V for 60 min at room temperature in dark. Electrophoretic mobility shift assay gels were analyzed and images were captured using the LI-COR Odyssey infrared laser imaging system.

Statistical analysis. All statistical analyses were carried out with SigmaStat software 3.5 (Systat Software). Quantitative data are presented as mean \pm SE. Control and respective IP6-treated groups were compared by one-way ANOVA followed by Bonferroni *t* test for multiple comparisons. $P < 0.05$ was considered statistically significant.

Results

IP6 inhibits growth and induces apoptosis in PC-3 cells. Earlier dose-response studies with IP6 have shown that 1 to 2 mmol/L concentrations exert the optimal antiproliferative and proapoptotic responses in different cancer cell lines (19–21, 26); accordingly, we selected 2 mmol/L IP6 concentration for all *in vitro* experiments. As shown in Fig. 1A, IP6 treatment moderately decreased the total cell number in 6 h (16%) and 12 h (26%) but had a relatively stronger effect at 24 h (42%; $P < 0.001$). On the other hand, IP6 caused a significant cell death beginning 6 h (4.6-fold; $P < 0.001$), which sustained at later time points of 12 and 24 h with 4.8-fold ($P < 0.002$) and 3.6-fold ($P < 0.001$) induction, respectively, compared with respective controls (Fig. 1A). Next, we assessed whether the IP6-caused cell death is apoptotic in nature and found that IP6 increases the apoptotic population of PC-3 cells by 2.4-fold ($P < 0.001$) and 4.3-fold ($P < 0.001$) at 6 and 12 h, respectively, and by 2.1-fold ($P < 0.005$) at 24 h (Fig. 1B). Consistent with these

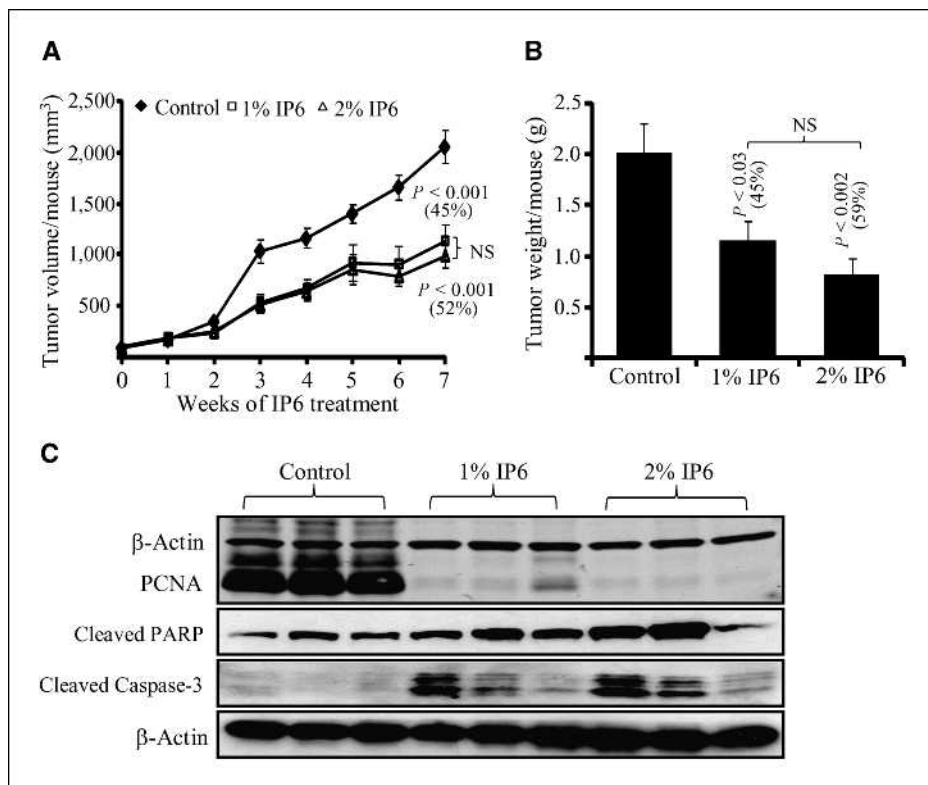


Figure 3. IP6 inhibits PC-3 tumor xenograft growth in nude mice together with *in vivo* antiproliferative and proapoptotic effects. PC-3 cells were s.c. injected on the right flank of each mouse, 1% or 2% (w/v) IP6 was given in drinking water, and tumor volume was recorded as detailed in Materials and Methods. The average tumor volume is shown for the corresponding week (A), and tumor weight (g) per mouse (B) was noted at the end of the study. Control and respective IP6-treated groups were compared by one-way ANOVA followed by Bonferroni *t* test for multiple comparisons. $P < 0.05$ was considered statistically significant. C, tumor cell lysates were prepared and Western blot analysis was done as detailed in Materials and Methods to assess the effect of IP6 on proliferation (proliferating cell nuclear antigen) and apoptosis (cleaved PARP and cleaved caspase-3). NS, statistically not significant.

results, immunoblot analysis showed a strong time-dependent increase in cleaved PARP levels as well as prominent upregulation of cleaved caspase-3 in PC-3 cells treated with IP6 for 6 and 12 h (Fig. 1C). Together, these results showed that IP6 inhibits growth and induces caspase-dependent apoptotic death in PC-3 cells.

IP6 decreases phosphorylation or expression of signaling molecules in PI3K-Akt axis. PI3K signaling pathway is constitutively activated in most of the prostate cancer cells, including PC-3 and C4-2B, due to altered expression/function of tumor suppressor PTEN (27); therefore, we next analyzed the effect of IP6 on different elements of PI3K-Akt pathway. The regulatory subunit of PI3K (p85) was used to determine the protein level and activation of PI3K, whereas the activation of PDK1 was assessed by its phosphorylation at Ser²⁴¹ (28). As shown in Fig. 2A, IP6 strongly decreased the phosphorylated levels of p85 at Tyr⁴⁵⁸ and PDK1 at Ser²⁴¹ without any changes in total p85 and PDK1 protein levels in PC-3 cells. Studies in the past decade have established that PI3K-Akt signaling plays a critical role in maintaining continued proliferation of prostate cancer cells where ILK can directly phosphorylate both Akt (Ser⁴⁷³) and GSK3 β and thereby inhibit apoptosis and facilitate cell survival (29–31). Consistent with its effect on PI3K and PDK1 phosphorylation, IP6 treatment of PC-3 cells caused a strong decrease in ILK1 protein levels (Fig. 2B) and a reduction in the phosphorylation of Akt at Ser⁴⁷³ and Thr³⁰⁸ sites and GSK3 α/β at Ser²¹ and Ser⁹ at all treatment times (Fig. 2B). Previous studies have shown that ILK-overexpressing cells have a high level of cyclin D1 (32) and knocking down ILK reduces it (6). Consistent with these findings and our own results showing IP6 effect on PI3K-Akt axis, we observed a lower protein expression of cyclin D1 with IP6 treatment of PC-3 cells at all time points (Fig. 2B). Because human prostate cancer is now considered to be largely due to cancer cells that harbor androgen receptor irrespective of

androgen dependence, we expanded PC-3 cells results in C4-2B cells that represent human prostate cancer carrying functional androgen receptor without androgen independence (33). As shown in Fig. 2, similar IP6 treatments of C4-2B cells produced comparable effects on the molecules in PI3K-Akt axis as in PC-3 cells. Together, these observations strongly suggest that IP6 impairs PI3K-PDK1-ILK1-Akt pathway and subsequent downstream events as a broad general effect in human prostate cancer cells.

IP6 inhibits PC-3 tumor xenograft growth in nude mice together with *in vivo* antiproliferative and proapoptotic effects. Earlier studies have shown IP6 activity in inhibiting the growth of various prostate cancer cells *in vitro* and *in vivo* under different treatment regimens (19–24, 26). However, based on our *in vitro* findings in the present study showing inhibition of PI3K-Akt pathway by IP6 and its plausible association with apoptotic response in PC-3 cells, we extended our studies to an *in vivo* xenograft model to validate the significance of our *in vitro* findings. A week after the inoculation of PC-3 cells, mice were fed with 1% or 2% (w/v) IP6 in drinking water until the completion of the experiment. We did not observe any significant change in body weight, diet consumption, and water intake (data not shown) or any adverse effects in terms of general behavior of animals fed with IP6 compared with the control animals throughout the experiment. Regarding its anticancer efficacy, IP6 treatments at 1% and 2% in drinking water started showing an inhibition in tumor growth by 2 weeks of treatment, which became more visible and statistically significant ($P < 0.001$) at the end of third week (Fig. 3A). By study end (seventh week), tumor volume per mouse decreased from $2,051 \pm 157 \text{ mm}^3$ in control group to $1,120 \pm 168$ and $979 \pm 115 \text{ mm}^3$ in 1% and 2% IP6-fed groups, respectively, accounting for 45% ($P < 0.001$) and 52% ($P < 0.001$) inhibition in tumor growth (Fig. 3A). Tumor weight results at study end further supported these findings where, compared with control group with tumor weight of $2.0 \pm 0.28 \text{ g/mouse}$, 1%

and 2% IP6-fed mice had 1.1 ± 0.19 and 0.8 ± 0.16 g/mouse tumor weights, respectively, accounting for 45% ($P < 0.02$) and 59% ($P < 0.001$) decrease (Fig. 3B). The *in vivo* significance of cell culture findings related to growth inhibition and apoptosis induction and their association with PC-3 tumor growth inhibition by IP6 were next established using tumor xenografts. We observed that both doses of IP6 strongly inhibited the protein levels of proliferating cell nuclear antigen and induced the levels of cleaved caspase-3 and cleaved PARP (Fig. 3C), supporting antiproliferative and proapoptotic effects of IP6.

IP6 strongly decreases the expression of ILK1, pAkt (Ser⁴⁷³), and cyclin D1 in PC-3 tumor xenografts. Overexpression of ILK in epithelial cells leads to enhanced anchorage-independent cell growth, cell cycle progression, and constitutive upregulation of cyclins D1 and A, suggesting ILK to be a proto-oncogene (14). Microscopic analysis of ILK1 immunostaining intensity showed 42% ($P < 0.001$) and 61% ($P < 0.001$) reduction in PC-3 tumor xenografts from 1%

and 2% IP6-treated mice, respectively, compared with controls (Fig. 4A-D). Downstream of ILK, activation of Akt is a poor prognostic factor in prostate cancer. Kreisberg and colleagues have shown that phosphorylation of Akt is often superior to Gleason grading for predicting biochemical recurrence of prostate cancer following radical prostatectomy (34). Immunohistochemical analysis of the tumor sections showed that 1% IP6 primarily reduces nuclear staining of pAkt (30% reduction versus control; $P < 0.012$), whereas 2% IP6 significantly reduced both nuclear (46% reduction versus control; $P < 0.001$) and cytoplasmic (~44% reduction versus control; $P < 0.001$; the quantitative data for cytoplasmic pAkt are not shown in figure) staining of pAkt (Fig. 4E-H). Consistent with the expression patterns of ILK1 and pAkt, quantification of cyclin D1 immunostaining showed 38% ($P < 0.002$) and 62% ($P < 0.001$) reduction in cyclin D1-positive cells with 1% and 2% IP6 treatment, respectively, compared with the controls (Fig. 4I-L).

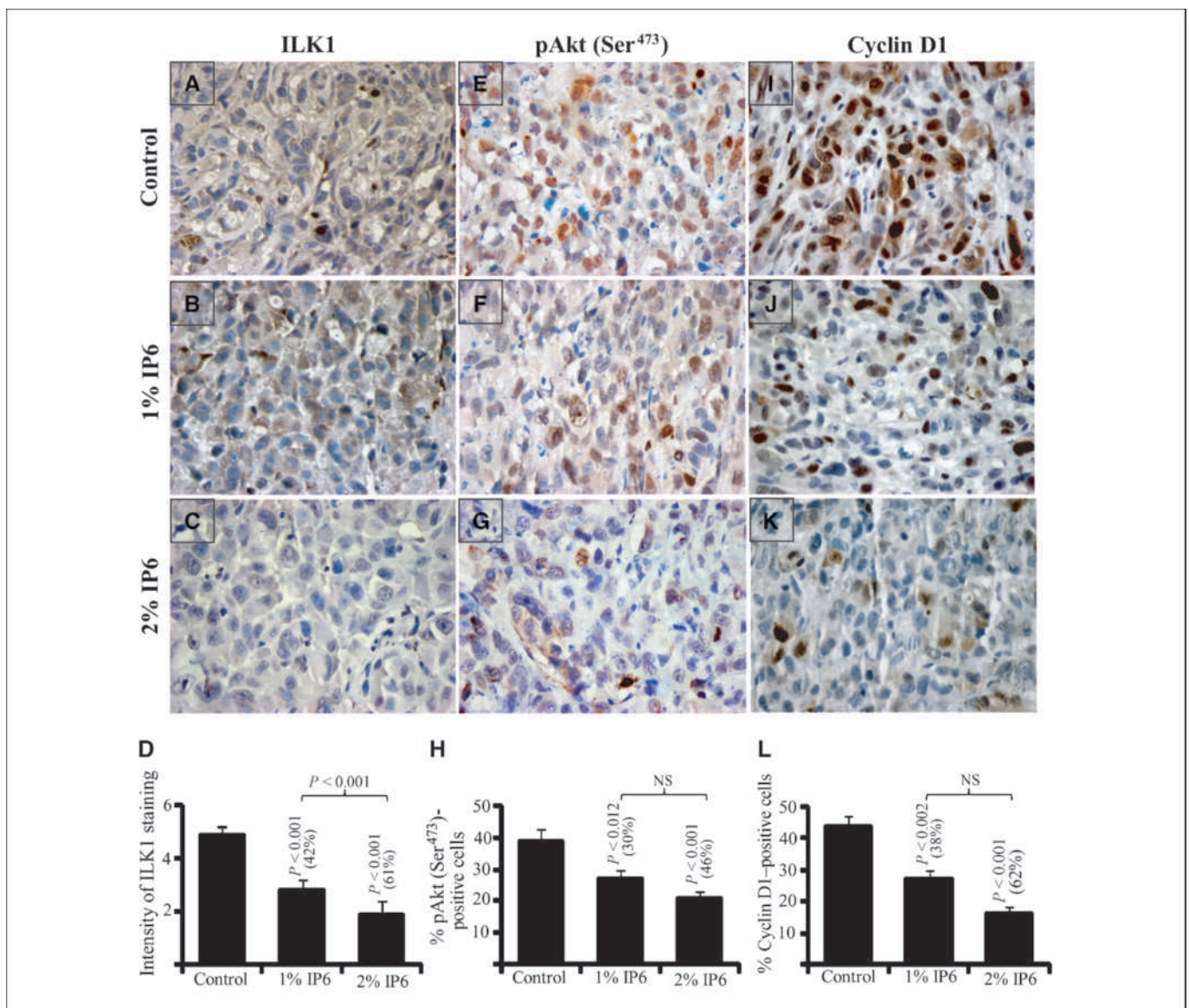


Figure 4. IP6 strongly decreases the expression of ILK1, pAkt (Ser⁴⁷³), and cyclin D1 in PC-3 tumor xenografts. Xenograft tissue samples from different treatment groups were subjected to immunohistochemical staining as detailed in Materials and Methods and analyzed qualitatively and quantitatively for the expression of ILK1 (A-D), nuclear pAkt-Ser⁴⁷³ (E-H), and cyclin D1 (I-L). In each case, the quantitative data are mean \pm SE of five tumor samples from an individual mouse in each group.

IP6 inhibits angiogenesis and decreases VEGF and eNOS expression in PC-3 tumor xenografts. CD31, an endothelial cell surface marker, serves as a reliable tool for the presence of microcapillaries in tumors (35). A significant inhibition in tumor growth with IP6 administration and a well-established role of Akt activation in angiogenesis also prompted us to assess the effect of IP6 on tumor vascularization using CD31 immunostaining. IP6 feeding at 1% and 2% IP6 doses decreased CD31⁺ microvessels by 35% ($P < 0.001$) and 57% ($P < 0.001$), respectively, compared with controls (Fig. 5A-D). To understand the mechanistic aspects of this antiangiogenic response of IP6, we analyzed the expression levels of VEGF and eNOS. It is well established that Akt stimulates VEGF production in tumor cells, which on secretion increases eNOS activity of both tumor and endothelial cells thereby leading to increased NO production. NO regulates various signaling pathways resulting in increased proliferation, angio-

genesis, and migration of tumor cells (36). Immunohistochemical analysis of the tumor sections showed that VEGF staining intensity in cytoplasm decreased by 36% ($P < 0.005$) and 47% ($P < 0.001$) with 1% and 2% IP6 treatment, respectively, compared with controls (Fig. 5E-H). More importantly, the intensity of eNOS immunostaining was reduced by 49% ($P < 0.001$) and 72% ($P < 0.001$) with 1% and 2% IP6 treatment, respectively, compared with controls (Fig. 5I-L). Together, these findings indicate that IP6 treatment exerts potent antiangiogenic response *in vivo* in PC-3 tumor xenografts by inhibiting the expression of proangiogenic factor VEGF and subsequent NO-mediated signaling events possibly by an upstream inhibitory effect on PI3K pathway.

IP6 strongly decreases HIF-1 α DNA-binding activity in PC-3 tumor xenografts. HIF-1 α is activated under hypoxic conditions and by various oncogenic signaling including mitogen-activated

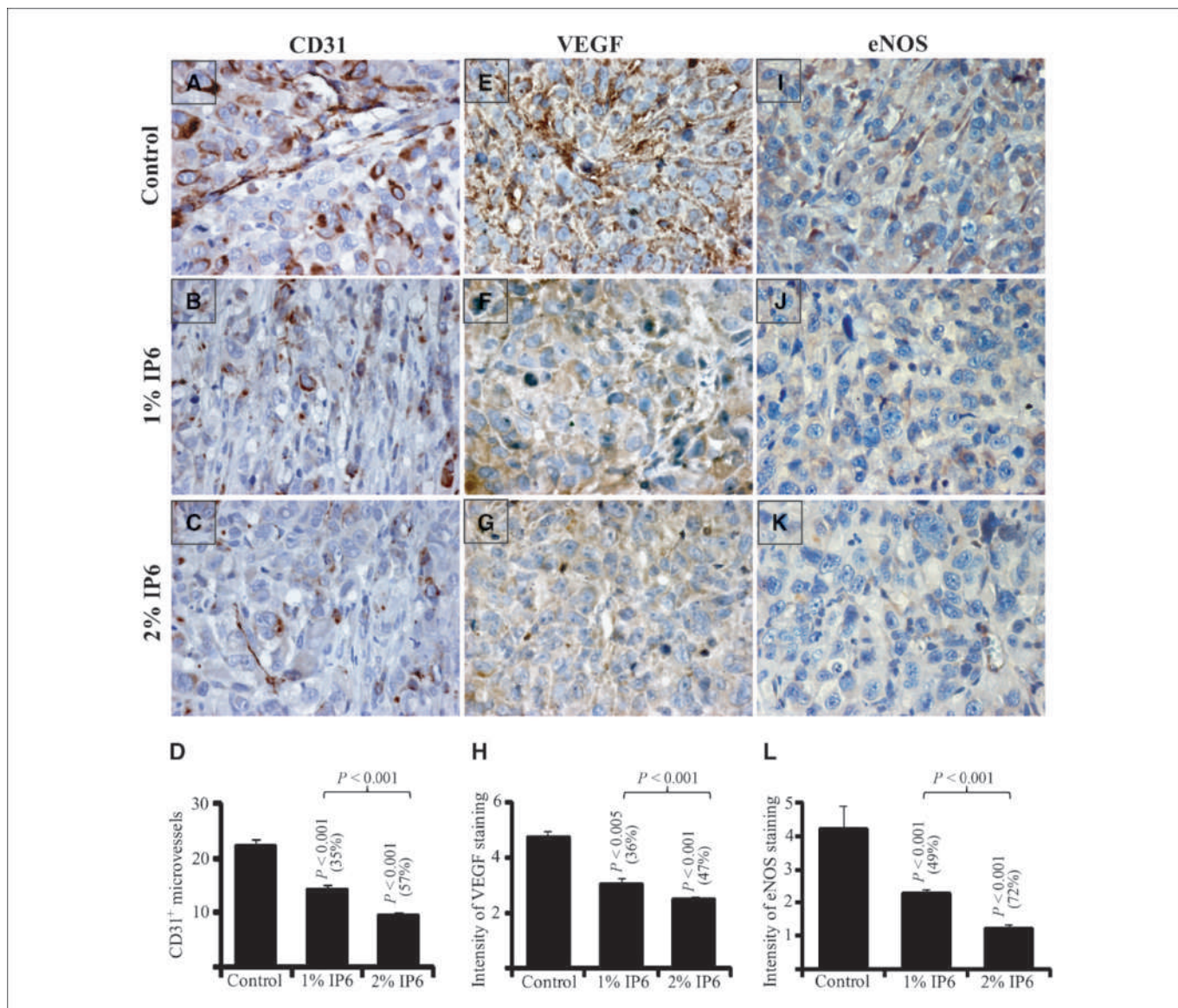


Figure 5. IP6 inhibits angiogenesis and decreases VEGF and eNOS expression in PC-3 tumor xenografts. Xenograft tissue samples from different treatment groups were subjected to immunohistochemical staining as detailed in Materials and Methods and analyzed qualitatively and quantitatively for CD31⁺ microvessels (A-D) and intensity of VEGF (E-H) and eNOS (I-L) immunostaining. In each case, the quantitative data are mean \pm SE of five tumor samples from an individual mouse in each group.

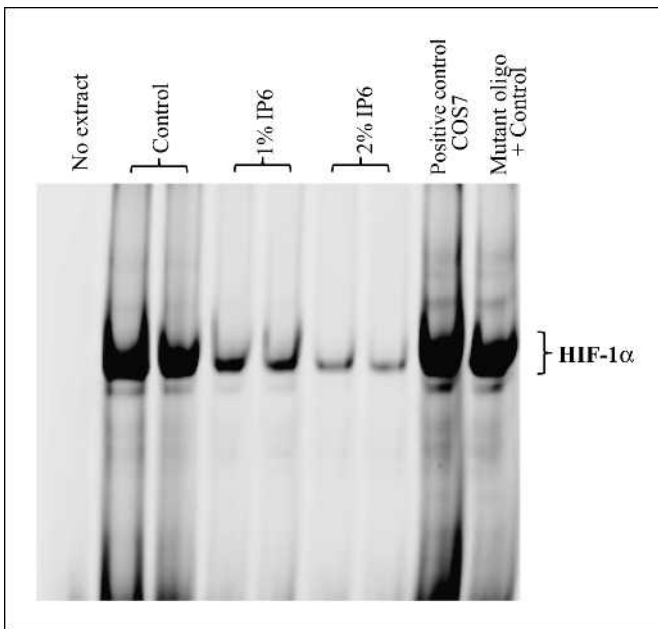


Figure 6. IP6 strongly decreases HIF-1 α DNA-binding activity in PC-3 tumor xenografts. Nuclear fractions were prepared from the tumor tissues and DNA-binding reactions were done for 30 min in the dark as per the manufacturer's instructions. The reaction mixture was resolved on 4% to 16% native bis-Tris gel and run at 100 V for 60 min at room temperature in the dark, and electrophoretic mobility shift assay gel was analyzed and images were captured using the LI-COR Odyssey infrared laser imaging system. COS7 (CoCl₂-treated) nuclear extract was used as positive control. Mutant HIF-1 IRDye end-labeled oligo was used to compete with the wild-type HIF-1 binding sequence along with the nuclear extract to establish the specificity of DNA-protein complex. Representative of three independent experiments.

protein kinase and PI3K pathways during tumor progression (37). On activation, HIF-1 α heterodimerizes with HIF-1 β and transcribes for various genes involved in metabolism, angiogenesis, and metastasis (38). Overexpression of HIF-1 α is observed in prostate tumors that have progressed from androgen-dependent to androgen-independent state and has been correlated with faster tumor growth and higher metastatic potential (39). It is also shown that the expression of HIF-1 α target genes, VEGF and insulin-like growth factor-II, increases in serum-starved prostate cancer cells and that the suppression of HIF-1 α expression significantly inhibits induced levels of VEGF and insulin-like growth factor-II (38). In our cell culture studies, PC-3 cells grown in normal conditions did not show HIF-1 α protein accumulation (data not shown); we did not manipulate serum conditions and/or growth factor treatments in these studies to artificially manipulate HIF-1 α protein accumulation and/or activation. Importantly, under the hypoxic microenvironment of PC-3 tumor xenograft growth in nude mice, we observed a strong HIF-1 α DNA-binding activity in the tumor tissues from control mice (Fig. 6). A prominent dose-dependent decrease in HIF-1 α DNA-binding activity, however, was clearly evident in the PC-3 tumor xenograft samples from both 1% and 2% IP6-fed nude mice (Fig. 6). Overall, these results indicate that IP6 strongly decreases HIF-1 α protein accumulation and its subsequent DNA-binding activity via inhibition of the PI3K-PDK1-ILK1-Akt pathway and thereby inhibits tumor vascularization.

Discussion

The present study for the first time reveals that a phytonutrient IP6 has prominent inhibitory effect on the PI3K-ILK1-Akt signaling

pathway, which accounts for its *in vitro* and *in vivo* growth-inhibitory, apoptotic, and antiangiogenic responses in highly invasive androgen-independent human prostate carcinoma PC-3 cells. PI3K-Akt pathway is an attractive therapeutic target in prostate cancer because modulation of various members of this pathway, including loss of PTEN function, significantly affects this malignancy. For instance, hypomorphic mutation of PDK1 significantly delays the onset of tumorigenesis in PTEN^{+/-} mouse model (40). Moreover, ILK is constitutively activated in PTEN-null prostate cancer cells and inhibition of ILK in these cells results in the lower expression of constitutively activated Akt (41). The present study identifies the strong inhibitory effect of IP6 on the phosphorylation (activation) of PI3K and its downstream signaling targets, PDK1 (Ser²⁴¹), ILK1, Akt (Thr³⁰⁸ and Ser⁴⁷³), and GSK3 α/β (Ser^{21/9}), in PTEN-null PC-3 cells.

Active cytosolic Akt has several direct targets that regulate cell cycle; for example, phosphorylation of GSK3, BAD, and p27 by Akt results in their inactivation causing increased cell survival and cell cycle progression. Moreover, nuclear Akt causes phosphorylation and nuclear exclusion of FOXO3A transcription factor, which therefore fails to transcribe for genes such as p27 (42). Immunohistochemical analysis of pAkt (Ser⁴⁷³) in PC-3 tumor xenografts showed that 1% IP6 primarily reduces nuclear expression, whereas 2% IP6 significantly reduces both nuclear and cytoplasmic expression of pAkt, which might account for the greater biological effect observed with the higher dose of IP6. GSK3 is widely reported to exert tumor suppressor function by inhibiting proliferation and inducing apoptosis; however, GSK3 has been shown to play a positive role in prostate tumor progression (43). Recently, Vene and colleagues showed that inhibition of GSK3 activity sensitizes prostate cancer cells to the apoptotic effect of triterpenoid CDDO-Me (44). This dual biological activity of GSK3 has also been shown to be dependent on cell type and stimulus (45). In our present study, a decreased GSK3 phosphorylation in PC-3 cells with IP6 treatment was associated with increased cell death indicating its proapoptotic role. An excessive rate of cyclin D1 production promotes cell cycle progression even in androgen- or serum-deprived prostate cancer cells (46). Molecular analysis of PC-3 tumor xenografts showed that the observed strong inhibitory effect of IP6 feeding on tumor growth was associated with lower levels of proliferating cell nuclear antigen and cyclin D1 and a marked induction in cleaved PARP and caspase-3, supporting the notion that inhibition of PI3K-Akt pathway by IP6 decreases both survival and proliferation and initiates apoptotic death.

Clinical studies have indicated the promise of antiangiogenic therapy in the management of prostate cancer (47). One of the key mediators of angiogenesis is VEGF, which promotes proliferation, survival, and migration of endothelial cells (48). ILK stimulates VEGF expression via Akt and HIF-1 α , and inhibition of ILK expression or activity in DU145 and PC-3 cells results in a dramatic decrease in VEGF expression (16). In our present study, IP6 treatment strongly decreased ILK1 expression, inhibited Akt phosphorylation, and possibly arrested the development of microcapillaries in PC-3 tumor xenografts as evidenced by decreased CD31 immunostaining. Reduced angiogenesis, therefore, might be partially responsible for the reduced tumor size in IP6-treated mice. Because Akt-dependent activation of eNOS stimulates angiogenesis and is also responsible for tumor maintenance (49), the considerable decreased expression of eNOS in IP6-treated PC-3 tumor xenografts provides additional support that inhibition of PI3K-Akt-eNOS signaling is a significant mechanism by which IP6 mediates its

antiproliferative and antiangiogenic response *in vivo*. HIF-1 α is one of the major transcriptional regulators of VEGF and is overexpressed in human prostate cancer cells (50). Our results indicate that inhibition of PI3K-Akt signaling by IP6 led to a decreased HIF-1 transcriptional activity, which possibly resulted in decreased VEGF secretion, eventually leading to the reduction in vascularization and impeded tumor growth.

In conclusion, our findings clearly show that IP6 inhibits PI3K-PDK1-ILK1-Akt-mediated signaling pathway and produces strong antitumor activity in advanced and aggressive human prostate cancer PC-3 xenografts by inhibiting proliferation and angiogenesis together with increased apoptosis. These observations suggest that

IP6 should be considered for its clinical efficacy against prostate cancer.

Disclosure of Potential Conflicts of Interest

No potential conflicts of interest were disclosed.

Acknowledgments

Received 7/29/09; revised 9/27/09; accepted 10/8/09; published OnlineFirst 11/17/09.
Grant support: National Cancer Institute RO1 grant CA116636.

The costs of publication of this article were defrayed in part by the payment of page charges. This article must therefore be hereby marked *advertisement* in accordance with 18 U.S.C. Section 1734 solely to indicate this fact.

References

- Damber JE, Aus G. Prostate cancer. *Lancet* 2008;371:1710-21.
- Gilligan T, Kantoff PW. Chemotherapy for prostate cancer. *Urology* 2002;60:94-100; discussion.
- Zellweger T, Gasser T. How to treat a localized prostate cancer: irradiation, surgery or watchful waiting? *Praxis (Bern 1994)* 2005;94:1307-8.
- Vanhaesebroeck B, Alessi DR. The PI3K-PDK1 connection: more than just a road to PKB. *Biochem J* 2000;346:561-76.
- Cruet-Hennequart S, Maubant S, Luis J, Gauduchon P, Staedel C, Dedhar S. α , integrins regulate cell proliferation through integrin-linked kinase (ILK) in ovarian cancer cells. *Oncogene* 2003;22:1688-702.
- Troussard AA, Mawji NM, Ong C, Mui A, St-Arnaud R, Dedhar S. Conditional knock-out of integrin-linked kinase demonstrates an essential role in protein kinase B/Akt activation. *J Biol Chem* 2003;278:22374-8.
- Yau CY, Wheeler JJ, Sutton KL, Hedley DW. Inhibition of integrin-linked kinase by a selective small molecule inhibitor, QLT0254, inhibits the PI3K/PKB/mTOR, Stat3, and FKHR pathways and tumor growth, and enhances gemcitabine-induced apoptosis in human orthotopic primary pancreatic cancer xenografts. *Cancer Res* 2005;65:1497-504.
- Manning BD, Cantley LC. AKT/PKB signaling: navigating downstream. *Cell* 2007;129:1261-74.
- Cross DA, Alessi DR, Cohen P, Andjelkovic M, Hemmings BA. Inhibition of glycogen synthase kinase-3 by insulin mediated by protein kinase B. *Nature* 1995;378:785-9.
- Srivastava AK, Pandey SK. Potential mechanism(s) involved in the regulation of glycogen synthesis by insulin. *Mol Cell Biochem* 1998;182:135-41.
- Diehl JA, Cheng M, Roussel MF, Sherr CJ. Glycogen synthase kinase-3 β regulates cyclin D1 proteolysis and subcellular localization. *Genes Dev* 1998;12:3499-511.
- Mulholland DJ, Dedhar S, Wu H, Nelson CC. PTEN and GSK3 β : key regulators of progression to androgen-independent prostate cancer. *Oncogene* 2006;25:329-37.
- Peifer C, Alessi DR. Small-molecule inhibitors of PDK1. *ChemMedChem* 2008;3:1810-38.
- Radeva G, Petrocelli T, Behrend E, et al. Overexpression of the integrin-linked kinase promotes anchorage-independent cell cycle progression. *J Biol Chem* 1997;272:13937-44.
- Graff JR, Deddens JA, Konicek BW, et al. Integrin-linked kinase expression increases with prostate tumor grade. *Clin Cancer Res* 2001;7:1987-91.
- Tan C, Cruet-Hennequart S, Troussard A, et al. Regulation of tumor angiogenesis by integrin-linked kinase (ILK). *Cancer Cell* 2004;5:79-90.
- Bakewell S. Phytic acid: a phytochemical with complementary and alternative benefits. *Cancer Biol Ther* 2006;5:1134-5.
- Vucenik I, Shamsuddin AM. Protection against cancer by dietary IP6 and inositol. *Nutr Cancer* 2006;55:109-25.
- Agarwal C, Dhanalakshmi S, Singh RP, Agarwal R. Inositol hexaphosphate inhibits growth and induces G₁ arrest and apoptotic death of androgen-dependent human prostate carcinoma LNCaP cells. *Neoplasia* 2004;6:646-59.
- Singh RP, Agarwal C, Agarwal R. Inositol hexaphosphate inhibits growth, and induces G₁ arrest and apoptotic death of prostate carcinoma DU145 cells: modulation of CDK1-CDK-cyclin and pRb-related protein-E2F complexes. *Carcinogenesis* 2003;24:555-63.
- Shamsuddin AM, Yang GY. Inositol hexaphosphate inhibits growth and induces differentiation of PC-3 human prostate cancer cells. *Carcinogenesis* 1995;16:1975-9.
- Roy S, Gu M, Ramasamy K, et al. p21/Cip1 and p27/Kip1 are essential molecular targets of inositol hexaphosphate for its antitumor efficacy against prostate cancer. *Cancer Res* 2009;69:1166-73.
- Singh RP, Sharma G, Mallikarjuna GU, Dhanalakshmi S, Agarwal C, Agarwal R. *In vivo* suppression of hormone-refractory prostate cancer growth by inositol hexaphosphate: induction of insulin-like growth factor binding protein-3 and inhibition of vascular endothelial growth factor. *Clin Cancer Res* 2004;10:244-50.
- Raina K, Rajamanickam S, Singh RP, Agarwal R. Chemopreventive efficacy of inositol hexaphosphate against prostate tumor growth and progression in TRAMP mice. *Clin Cancer Res* 2008;14:3177-84.
- Gu M, Singh RP, Dhanalakshmi S, Agarwal C, Agarwal R. Silibinin inhibits inflammatory and angiogenic attributes in photocarcinogenesis in SKH-1 hairless mice. *Cancer Res* 2007;67:3483-91.
- Diallo JS, Peant B, Lessard L, et al. An androgen-independent androgen receptor function protects from inositol hexakisphosphate toxicity in the PC3/PC3(AR) prostate cancer cell lines. *Prostate* 2006;66:1245-56.
- Davies MA, Koul D, Dhese H, et al. Regulation of Akt/PKB activity, cellular growth, and apoptosis in prostate carcinoma cells by MMAC/PTEN. *Cancer Res* 1999;59:2551-6.
- Stambolic V, Suzuki A, de la Pompa JL, et al. Negative regulation of PKB/Akt-dependent cell survival by the tumor suppressor PTEN. *Cell* 1998;95:29-39.
- Casamayor A, Morrice NA, Alessi DR. Phosphorylation of Ser-241 is essential for the activity of 3-phosphoinositide-dependent protein kinase-1: identification of five sites of phosphorylation *in vivo*. *Biochem J* 1999;342:287-92.
- Persad S, Attwell S, Gray V, et al. Inhibition of integrin-linked kinase (ILK) suppresses activation of protein kinase B/Akt and induces cell cycle arrest and apoptosis of PTEN-mutant prostate cancer cells. *Proc Natl Acad Sci U S A* 2000;97:3207-12.
- Troussard AA, Tan C, Yoganathan TN, Dedhar S. Cell-extracellular matrix interactions stimulate the AP-1 transcription factor in an integrin-linked kinase- and glycogen synthase kinase 3-dependent manner. *Mol Cell Biol* 1999;19:7420-7.
- D'Amico M, Hulit J, Amanatullah DF, et al. The integrin-linked kinase regulates the cyclin D1 gene through glycogen synthase kinase 3 β and cAMP-responsive element-binding protein-dependent pathways. *J Biol Chem* 2000;275:32649-57.
- Ko S, Shi L, Kim S, Song CS, Chatterjee B. Interplay of nuclear factor- κ B and B-myb in the negative regulation of androgen receptor expression by tumor necrosis factor α . *Mol Endocrinol* 2008;22:73-86.
- Kreisberg JI, Malik SN, Prihoda TJ, et al. Phosphorylation of Akt (Ser⁴⁷³) is an excellent predictor of poor clinical outcome in prostate cancer. *Cancer Res* 2004;64:5232-6.
- Woodfin A, Voisin MB, Nourshargh S. PECAM-1: a multi-functional molecule in inflammation and vascular biology. *Arterioscler Thromb Vasc Biol* 2007;27:2514-23.
- Fukumura D, Kashiwagi S, Jain RK. The role of nitric oxide in tumour progression. *Nat Rev Cancer* 2006;6:521-34.
- Blancher C, Moore JW, Robertson N, Harris AL. Effects of ras and von Hippel-Lindau (VHL) gene mutations on hypoxia-inducible factor (HIF)-1 α , HIF-2 α , and vascular endothelial growth factor expression and their regulation by the phosphatidylinositol 3'-kinase/Akt signaling pathway. *Cancer Res* 2001;61:7349-55.
- Kapitsinou PP, Haase VH. The VHL tumor suppressor and HIF: insights from genetic studies in mice. *Cell Death Differ* 2008;15:650-9.
- Hao P, Chen X, Geng H, Gu L, Chen J, Lu G. Expression and implication of hypoxia inducible factor-1 α in prostate neoplasm. *J Huazhong Univ Sci Technol Med Sci* 2004;24:593-5.
- Bayasas JR, Leslie NR, Parsons R, Fleming S, Alessi DR. Hypomorphic mutation of PDK1 suppresses tumorigenesis in PTEN(+/-) mice. *Curr Biol* 2005;15:1839-46.
- Persad S, Attwell S, Gray V, et al. Regulation of protein kinase B/Akt-serine 473 phosphorylation by integrin-linked kinase: critical roles for kinase activity and amino acids arginine 211 and serine 343. *J Biol Chem* 2001;276:27462-9.
- Huang H, Tindall DJ. Dynamic FoxO transcription factors. *J Cell Sci* 2007;120:2479-87.
- Liao X, Thrasher JB, Holzbeierlein J, Stanley S, Li B. Glycogen synthase kinase-3 β activity is required for androgen-stimulated gene expression in prostate cancer. *Endocrinology* 2004;145:2941-9.
- Vene R, Larghero P, Arena G, Sporn MB, Albini A, Tosetti F. Glycogen synthase kinase 3 β regulates cell death induced by synthetic triterpenoids. *Cancer Res* 2008;68:6987-96.
- Patel S, Woodgett J. Glycogen synthase kinase-3 and cancer: good cop, bad cop? *Cancer Cell* 2008;14:351-3.
- Chen Y, Martinez LA, LaCava M, Coghlan L, Conti CJ. Increased cell growth and tumorigenicity in human prostate LNCaP cells by overexpression to cyclin D1. *Oncogene* 1998;16:1913-20.
- Aragon-Ching JB, Dahut WL. The role of angiogenesis inhibitors in prostate cancer. *Cancer J* 2008;14:20-5.
- Ferrara N. VEGF and the quest for tumour angiogenesis factors. *Nat Rev Cancer* 2002;2:795-803.
- Lim KH, Ancrile BB, Kashatus DF, Counter CM. Tumour maintenance is mediated by eNOS. *Nature* 2008;452:646-9.
- Zhou Q, Liu LZ, Fu B, et al. Reactive oxygen species regulate insulin-induced VEGF and HIF-1 α expression through the activation of p70S6K1 in human prostate cancer cells. *Carcinogenesis* 2007;28:28-37.